Targeting complement component 5a promotes vascular integrity and limits airway remodeling

Mohammad A. Khan[a], Christian Maasch[b], Axel Vater[b], Sven Klussmann[b], John Morser[a,c], Lawrence L. Leung[a,c], Carl Atkinson[d], Stephen Tomlinson[d], Peter S. Heeger[e], and Mark R. Nicolls[a,c,1]

[a]Medical Service, Veterans Affairs Palo Alto Health Care System, Palo Alto, CA 94304; [b]NOXXON Pharma, 10589 Berlin, Germany; [d]Department of Microbiology and Immunology, Medical University of South Carolina, Charleston, SC 29425; [e]Department of Medicine, Mount Sinai Hospital, New York, NY 10029; and [c]Department of Medicine, Stanford University School of Medicine, Stanford, CA 94305

Increased microvascular dilatation and permeability is observed during allograft rejection. Because vascular integrity is an important indicator of transplant health, we have sought to limit injury to blood vessels by blocking complement activation. Although complement component 3 (C3) inhibition is known to be vasculoprotective in transplantation studies, we recently demonstrated the paradoxical finding that, early in rejection, C3$^{-/-}$ transplant recipients actually exhibit worse microvascular injury than controls. In the genetic absence of C3, thrombin-mediated complement component 5 (C5) convertase activity leads to the generation of C5a (anaphylatoxin), a promoter of vasodilatation and permeability. In the current study, we demonstrated that microvessel thrombin deposition is significantly increased in C3$^{-/-}$ recipients during acute rejection. Thrombin colocalization with microvessels is closely associated with remarkably elevated plasma levels of C5a, vasodilatation, and increased vascular permeability. Administration of NOX-D19, a specific C5a inhibitor, to C3$^{-/-}$ recipients of airway transplants significantly improved tissue oxygenation, limited microvascular leakiness, and prevented airway ischemia, even in the absence of conventional T-cell–directed immunosuppression. As C3 inhibitors enter the clinics, the simultaneous targeting of this thrombin-mediated complement activation pathway and/or C5a itself may confer significant clinical benefit.

hypoxia | chronic rejection | alloimmunity | fibrosis | bronchiolitis obliterans syndrome

Microvascular loss during acute rejection episodes causes local tissue ischemia and probably contributes to fibrotic remodelling and organ dysfunction in transplant recipients (1–6). Lung transplant recipients may be especially vulnerable to this sort of injury because the bronchial arteries, the principal source of oxygenated blood in airways, are not usually reanastomosed at the time of surgery. The tenuous nature of this airway microcirculation prompted us to evaluate which immune components are chiefly responsible for causing tissue ischemia in functional orthotopic tracheal transplants. This model system faithfully replicates lymphocytic bronchitis, a large airway precursor of chronic rejection (bronchiolitis obliterans syndrome) (7). We demonstrated that either CD4 T-cell or antibody-triggered complement activity is independently sufficient to induce airway ischemia during allograft rejection, whereas CD8 T-cell activity is not (8). Although decreasing complement component 3 (C3) activity greatly reduces the duration of tissue ischemia associated with allograft rejection, it also paradoxically leads to vasodilatation, and increases microvessel permeability early in rejection. As C3 inhibitors are being increasingly considered for use in clinical medicine, including lung transplantation (9), it is important to address the unintended deleterious effects of this therapy.

Given our previous finding that microvessels in rejecting C3-deficient (C3$^{-/-}$) transplant recipients are both dilated and leaky (8), we questioned whether increasing levels of complement component 5a (C5a), a known anaphylatoxin, could account for the enhanced vasodilatation and permeability. In the absence of C3, a different complement activation pathway may lead to the generation of C5a in which thrombin substitutes for C3-dependent C5 convertase activity (10), and thrombin is notably elevated in acute allograft rejection (11). In the current study, we use the unique C5a inhibitor NOX-D19, a PEGylated 44 nucleotide L-RNA oligonucleotide (a so-called Spiegelmer) (12) that specifically binds to human and murine C5a and C5a-desArg. NOX-D19 also binds to C5a before its cleavage from human C5. The unnatural enantiomer of the ribose (L- instead of D-configuration) in the RNA-Spiegelmer increases its stability against attacks by RNases that are ubiquitous in biological fluids. Spiegelmers act like conventional aptamers by forming a 3D structure that binds with high affinity to the target of choice. A number of Spiegelmers have been generated by in vitro selection (13–15), and three Spiegelmers are currently being tested in clinical trials. The purpose of this study was to evaluate whether increased vascular thrombin was available to compensate for or to replace as a C5 convertase in a relevant in vivo model and to determine whether interrupting C5a activity through administration of the C5a inhibitor NOX-D19 would preserve microvascular function and airway architecture.

Results

Increased Thrombin Deposition on Vascular Endothelial Cells in Allografts in C3-Deficient Recipients Is Associated with Increased Systemic C5a Levels. C3$^{-/-}$ recipients of tracheal allografts exhibit improved graft perfusion over time because of enhanced neovascularization following acute rejection (8). However, during the first week of acute rejection, there is evidence of vasodilatation and increased permeability in allograft microvessels in C3$^{-/-}$ recipients (8). Although wild-type donor airways were a possible contributing source of complement, we did not detect significant vascular C3d in rejecting allografts of C3$^{-/-}$ recipients (Fig. S1). In plasma from C3$^{-/-}$ mice, a threefold elevation of thrombin activity, which can substitute for C3-dependent C5-convertase when incubated with human C5 ex vivo, has been reported (10). We found that airway allografts in C3$^{-/-}$ recipients exhibit significantly increased thrombin immunoreactivity that colocalizes with dilated microvessels at day 6 posttransplantation, several days before airway perfusion is lost (Fig. 1 *A*

IMMUNOLOGY

Fig. 1. Increased vascular thrombin in orthotopic tracheal transplants is associated with elevated plasma C5a. (*A*) Representative images showing colocalization of thrombin on CD31⁺ vascular endothelial cells (white arrows) on day 6 in allograft rejection in BALB/c →C57BL/6 grafts compared with BALB/c→C57BL/6 C3⁻/⁻ grafts. Yellow arrows point to dilated microvessels in C3⁻/⁻ group. E, epithelial layer; SE, subepithelial area in tracheal sections. Original magnification, 40×. (*B*) Morphometric assessments of thrombin/CD31⁺ colocalization. (*C*) Plasma levels of C5a in different groups evaluated on posttransplant days 4 and 8 ($n = 4$–6 per group). Data are shown as means with SEM. *$P < 0.05$. Group statistics are detailed in text.

and *B*). The specificity of the antithrombin antibody used is established by showing that thrombin staining is almost fully prevented by pretreatment of tracheal sections with hirudin. This finding also demonstrates that the thrombin active site is available because hirudin is a specific inhibitor of thrombin by binding to its active site (16). We hypothesized that a lack of C3b-mediated opsonization of damaged vascular intimal cells in C3⁻/⁻ recipients could lead to a prothrombotic endothelial surface and found that tissue factor, a protein necessary for the initiation of thrombin generation, also colocalized to microvessels in rejecting allografts (Fig. S2). Next, we assessed plasma C5a levels in C3⁻/⁻ recipients during allograft rejection and showed that C5a is significantly elevated to 2.7 ± 1.2 nM, $P = 0.01$ and 2.0 ± 0.10 nM, $P < 0.0001$ on day 4 and day 8, respectively, compared with C3⁺/⁺ recipients receiving allograft airways (Fig. 1*C*). Nongrafted mice exhibit C5a levels of 0.54 ± 0.23 nM and 0.43 ± 0.12 nM on day 4 and day 8, respectively. Syngrafted mice show slightly higher plasma levels of C5a with 1.0 ± 0.31 nM (day 4, $P < 0.05$) and 1.2 ± 0.11 nM (day 8, $P < 0.0001$) compared with nongrafted animals; values that are similar to wild-type allograft recipients. Therefore, active thrombin

appears to be available as a potential C5-convertase substitute at the site of relevant injury, generating the increased plasma C5a.

In C3⁻/⁻ Recipients, C5a Inhibition Prevents Increased Vascular Permeability in Rejecting Allografts. Because increased C5a levels appear to be associated with both the prominent vasodilatation and permeability in airway vessels of C3⁻/⁻ allograft recipients, we next sought to determine whether antagonizing C5a activity with the unique C5a inhibitor NOX-D19 could limit these vascular changes. NOX-D19 administration to C3⁻/⁻ recipients led to abrogated vasodilatation and diminished microsphere extravasation (Fig. 2). Of note, mildly increased vascular permeability is evident in wild-type (WT) rejection responses, and NOX-D19 therapy did not appear to eliminate this more limited microsphere egress from the airway circulation. Interestingly, NOX-D19 administration limited both vascular thrombin and tissue factor deposition during rejection, suggesting that C5a, itself, directly or indirectly contributed to the presence of these prothrombotic factors in damaged microvessels (Fig. S3). The vascular C5b-9 membrane attack complex is also relatively decreased in NOX-D19–treated recipients (Fig. S4). Finally, because C5 antagonism can attenuate alloimmune responses (17), we investigated the effects of NOX-D19 in rejecting airway allografts and found that treatment reduced vascular IgG deposition (Fig. S5) and T-cell infiltration (Fig. S6). Thus, inhibition with NOX-D19 appeared to block characteristic C5a-anaphylactoid actions on microvessels as well as inhibit the coagulation cascade, complement pathways, and alloimmune mediators, all factors that are potentially harmful to vascular integrity.
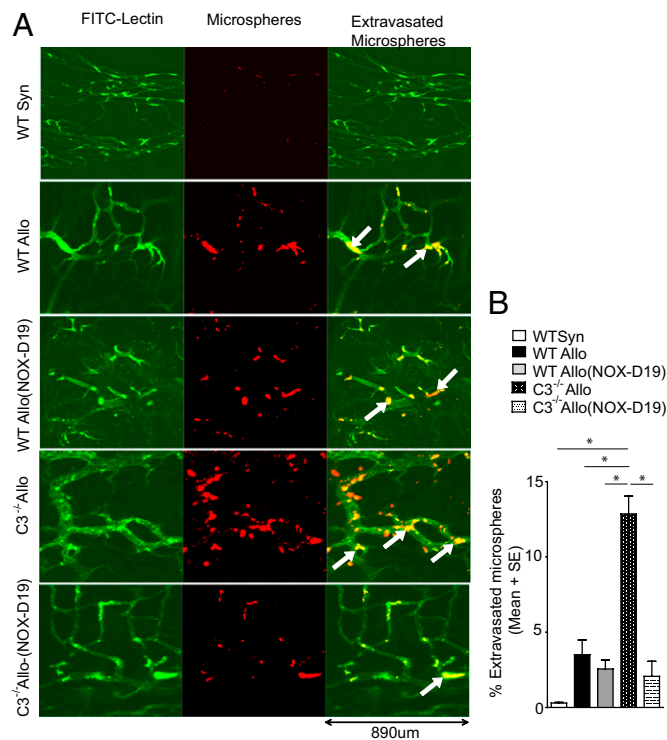
Fig. 2. C5a inhibition reduces graft vascular permeability and vasodilatation in C3⁻/⁻ recipients. (*A*) NOX-D19 treatment decreases microvessel permeability in C3⁻/⁻ recipients at d4 as demonstrated by FITC-lectin and R50 Fluoromax red microsphere localization in the microvasculature. Original magnification, 20×. (*B*) Morphometric assessment of microsphere extravasation in tracheal grafts on day 4 posttransplant ($n = 4$–6 per group). Data are shown as means with SEM, *$P < 0.05$.

C5a Inhibition Improves Graft Tissue pO$_2$ and Blood Perfusion in C3$^{-/-}$ Recipients. We next evaluated the effect of NOX-D19 on grafted airway tissue oxygenation and perfusion. We have previously reported that, whereas both C3 deficiency and inhibition of C3 convertase [with complement receptor 2–complement receptor 1-related gene/protein-y (CR2-Crry)] are associated with much briefer ischemic periods (due to greatly accelerated recipient-derived angiogenesis) (8), both groups paradoxically become ischemic a full 24 h before WT graft ischemia in early acute rejection. C3 deficiency and C3 convertase inhibition, in an essentially identical manner, are associated with early vascular compromise followed by accelerated revascularization via recipient-derived angiogenesis. We hypothesized that blocking C5a early in rejection would better prevent the profound tissue hypoxia and ischemia so closely associated with fibrotic remodeling. NOX-D19 treatment of C57BL/6 C3$^{-/-}$ mice, grafted with BALB/c tracheas, completely prevented severe tissue hypoxia and ischemia normally evident after nine days of rejection (Fig. 3). NOX-D19 monotherapy of WT recipients greatly reduced the duration, but did not fully prevent tissue hypoxia or ischemia, indicating C3-dependent vascular injury occurs in the absence of normal C5a activity. FITC-lectin perfusion studies, which identify functional microvessels, confirmed these findings (Fig. 4).

C5a Inhibition in C3$^{-/-}$ Recipients Prevents Collagen Deposition and Epithelial Transformation. We assessed the long-term impact of NOX-D19 treatment in C3$^{-/-}$ recipients by using PicroSirius red staining for collagen and morphological confocal assessments. Airway remodeling was prevented at day 28, even in the absence of T-cell–specific immunosuppression. C5a-inhibited C3$^{-/-}$ transplant recipients exhibit significantly less subepithelial collagen and display more preserved pseudostratified epithelium compared
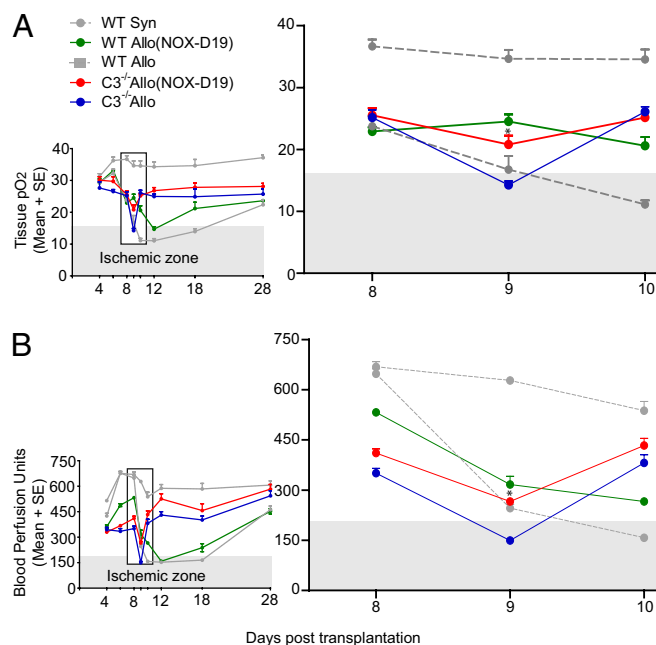
Fig. 3. C5a inhibition improves tissue pO$_2$ and blood perfusion in C3$^{-/-}$ recipients. (A) Tissue pO$_2$ (in mmHg) at different time points. The time scale of smaller insets is to facilitate examination of discrete time points, and the period of interest is expanded in larger graph on *Right*. (B) Blood perfusion to grafted airways on progressive days posttransplant ($n = 4$–6 animals per time point per group). The ischemic zone refers to the pO$_2$ and perfusion thresholds below which, the airway tissue is known to be nonperfused by FITC-lectin assessment. Data are shown as means with SEM. Day 9 C3$^{-/-}$ allograft (Allo) (NOX-D19) vs. C3$^{-/-}$ Allo *$P < 0.05$.
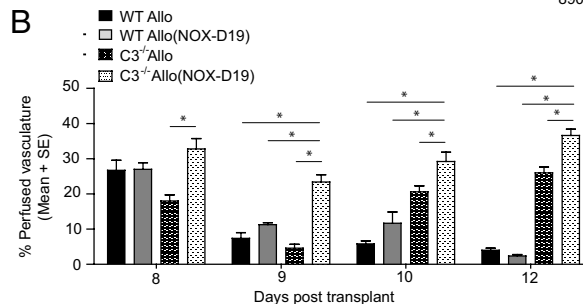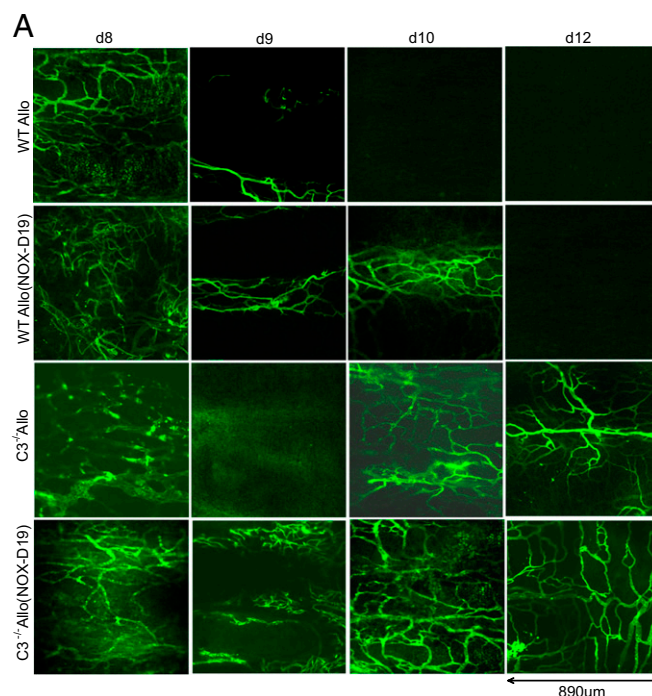

Fig. 4. C5a inhibition preserves microvascular flow in C3$^{-/-}$ recipients. (A) FITC-lectin perfusion profile of whole mounts tracheal grafts from d8 to d12 in C3$^{-/-}$ recipients and NOX-D19–treated recipients shows early recovery in microvascular flow during allograft rejection. Original magnification, 20×. (B) Morphometric assessments of perfused vasculature (FITC-lectin perfused vessels per unit area) in tracheal grafts at different time points ($n = 4$–6 animals per time point per group). Data are shown as means with SEM. *$P < 0.05$.

with NOX-D19–treated WT allografts (Fig. 5). This study provides in vivo evidence for C5 cleavage in the absence of a classical, C3b-containing C5 convertase and furthermore uniquely demonstrates, a unique clinical benefit of simultaneously limiting both C5a and C3 complement activity during alloimmune injury.

Discussion

In this study, we addressed the paradoxical finding of microvascular vasodilatation and leakiness previously observed in C3$^{-/-}$ and C3-inhibited recipients of allograft transplants (8). Vasodilatation and increased capillary permeability can be triggered by C5a, an anaphylatoxin. Given that the generation of thrombin is a well-established feature of both allograft and xenograft rejection (11, 18–20), we hypothesized that excessive C5a activation could occur if thrombin was substituting for C3-dependent C5 convertase at the graft site via a recently described complement activation pathway (10). We found that, in C3$^{-/-}$ mice, significantly increased thrombin deposits in graft microvessels are found in association with elevated systemic plasma concentrations of C5a. The histological specificity of vascular thrombin deposition is confirmed by hirudin, a specific thrombin inhibitor, blocking the
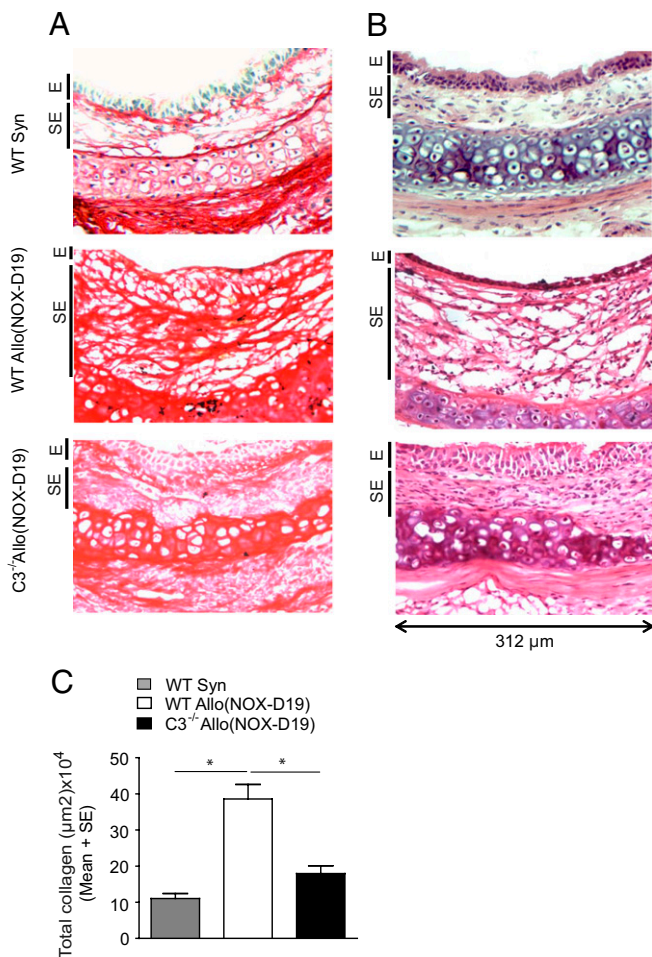
Fig. 5. NOX-D19–treated C3$^{-/-}$ recipients exhibit reduced collagen deposition and fibrotic remodeling. (*A*) Representative H&E images of orthotopic tracheal transplants 28 d posttransplantation. (*B*) Picrosirius red staining for collagen deposition on day 28. E and SE, graft epithelial and subepithelial areas, respectively. Original magnification, 40×. (*C*) Total collagen quantification for WT Syn, WT Allo vs. C3$^{-/-}$ Allo groups (*n* = 4–6 per group). Data are shown as means with SEM. *P < 0.05.

staining with antithrombin antibody. Of note, it has been previously demonstrated that systemic hirudin administration to rat cardiac allograft recipients attenuates graft arteriosclerosis in close association with reduced tissue factor expression in transplant vasculature; tissue factor being necessary for thrombin formation (21). The current study extends these observations by showing that thrombin itself colocalizes with the microvasculature: a finding that is, to our knowledge, a unique observation in transplant biology.

C3$^{-/-}$ recipients of allograft transplants exhibit the highest levels of plasma C5a, but milder elevations of the anaphylatoxin are also noted in WT recipients of allografts and syngrafts. To determine whether vasodilatation and leakiness in C3$^{-/-}$ recipients was attributable to C5a in these animals, we used a unique anti-C5a compound, Spiegelmer NOX-D19, and found that therapy with this agent prevents this microvascular pathology. Although thrombin can itself cause microvascular leaks, our data suggest that in this setting, the complement system and not thrombin is responsible. In addition to limiting alloimmune inflammation, NOX-D19 treatment also resulted in less overall vascular thrombin and tissue factor deposition, a finding that suggests that in C3-deficiency states a feed-forward mechanism occurs in which thrombin enhances C5a production, which, in

turn, leads to further tissue factor and thrombin generation in microvessels (modeled in Fig. S7). Further, the simultaneous loss of complement C3 and C5a activity is sufficient to completely prevent airway ischemia, even in the absence of other immunosuppression. Preservation of blood flow in the allograft is highly correlated with maintenance of normal airway architecture (5, 6, 8), and C5a-inhibited C3$^{-/-}$ recipients of tracheal allografts maintain normal airway architecture as defined by relatively little subepithelial fibrosis and normal pseudostratified epithelium.

The complement and coagulation systems are crucial components of innate immune responses that are jointly enlisted in the fight against foreign antigens (22); both systems appear to act in a coordinated and unique manner in the current study. During the early phase of inflammation, complement activation generates the complement fragments, C3a, C4a, and C5a which are all potent anaphylatoxins that alter vascular permeability. In normal circumstances, C3 plays a central role in generating C5 convertase to cleave C5 into active fragments. The mechanism accounting for observed enhanced generation of C5a in C3 deficiency remains undefined. We postulate that lack of opsonization of damaged microvasculature leads to impaired clearance of cell debris (23), increased expression of tissue factor, and activation of the coagulation cascade. Thrombin has been reported to be able to substitute for C5 convertase and activate C5 directly (10, 24, 25). However, recent studies indicate that direct activation of C5 by thrombin can occur but is inefficient; instead of cleaving C5 at the C5 convertase cleavage site, thrombin cleaves C5 at a unique site, generating a unique C5 cleavage product (C5b$_T$), which is further cleaved by C5 convertase, resulting in a C5b$_T$-9 membrane attack complex with enhanced lytic activity (26). Neutrophil elastase (27), plasmin, macrophage serine proteases (28), Factors Xa, IXa, and XIa (22) have all been reported to have C5 convertase activity. It is possible that thrombin, in combination with one of these enzymes, activates C5 in the absence of C3. C5a is the most potent anaphylatoxin (29), and its biological effects include basophil and mast cell degranulation, enhanced vascular permeability, and smooth muscle contraction (30, 31). C5a is a much more potent chemotactic agent than C3a and significantly contributes to the recruitment and activation of leukocytes (32, 33). Correspondingly, anti-C5a mAb synergizes with cytotoxic T-lymphocyte antigen 4 immunoglobulin (CTLA4Ig) to prolong cardiac allograft survival, in part, because it blocks the in vivo trafficking of primed T cells to the transplant (17). Several approaches have been used to eliminate the toxic effects of active C5 fragments including inhibiting C5 cleavage by inhibiting C5 cleavage via targeting the C5 molecule itself, blocking the activity of C5a by neutralizing antibodies and through the targeting of C5a receptors (31). In the current study, the clinical benefit of one such inhibitor, the C5a-targeting Spiegelmer NOX-D19, adds unique relevance to C5a antagonism as a possible combinational therapy with C3 antagonists. In addition to limiting leukocyte trafficking and activation, C5a inhibitors may uniquely stabilize blood vessels at risk.

Materials and Methods

Procedure of Orthotopic Tracheal Transplantation. The Veterans Affairs Palo Alto Animal Care and Use Committee approved experiments used in this study. Orthotopic tracheal transplants were prepared according to our established procedure as described previously with slight modifications (6, 8). All mice (4–6 wk) were purchased from the Jackson Laboratory. C3$^{-/-}$ mice (allele symbol/name: *C3^c*, fast electrophoretic mobility) were on a BL/6 (H-2^b) genetic background and were homozygous for the *C3* (complement component C3) targeted mutation. Recipients, C57BL/6 (H-2^b) wild-type and C3$^{-/-}$ (H-2^b) mice, were anesthetized with 120 mg/kg ketamine and 5 mg/kg xylazine and transplanted with tracheas (5–7 ring) removed from CO$_2$-euthanized donor C57BL/6 (syngeneic) or MHC-mismatched BALB/c (H-2^d) mice (allogeneic). After cutting the recipient trachea, the donor trachea was sewn in with 10-0 nylon sutures, and the overlying skin was closed with 5-0 silk sutures. After

the procedure, mice were given buprenorphine (0.1 mg/kg s.c.) for post-operative analgesia and baytril (5 mg/kg s.c.) for postoperative antibiosis.

C5a Inhibitor NOX-D19. A manuscript fully describing the discovery and detailed characterization of the anti-C5a Spiegelmer NOX-D19 is under preparation. Briefly, the oligonucleotide part of NOX-D19, a 44 nucleotide L-RNA was prepared by phosphoramidite solid phase synthesis and conjugated to NHS-activated (Y-shaped) 40-kDa methoxy PEG (Jenkem) via a 5′-aminohexyl linker.

NOX-D19 Administration. To study the effects of C5a antagonism, C57BL/6 WT (H-2[b]) allografts and C57BL/6 C3^{−/−} (H-2[b]) recipients grafted with BALB/c (H-2[d]) airway grafts were given 10 mg/kg i.p. of NOX-D19 or saline control at day 0 (d0) and every second day thereafter. NOX-D19–treated and saline-treated recipients were monitored at d4, d6, d8, d9, d10, d12, and d28 for graft tissue pO2 and blood perfusion. Microvascular permeability and collagen deposition was assessed at day 4 and day 28, respectively.

Quantification of Plasma C5a. To quantify C5a levels, blood was first collected through the venous eye plexus in lithium-heparin tubes and isolated by centrifuging aliquots at $1,200 \times g$ for 15 min. The Biacore 2000 instrument (GE Healthcare) was set to a constant temperature of 37 °C. For the quantification of C5a and C5a-desArg in murine plasma 8,000–9,000 response units (RU) of an anti-C5a antibody that has the same affinity to C5a-desArg were immobilized by a 1-ethyl-3-(3-dimethylaminopropyl)carbodiimide (EDC)/N-hydroxysuccinimide (NHS) covalent coupling procedure. An isotype control mAb was immobilized likewise on a control flow cell to monitor nonspecific binding. Regeneration between analyte injections was performed by injecting 15 µL of glycine-HCl pH 1.5. The plasma samples were diluted at 1:10 in measurement buffer; association and dissociation of the binding event were recorded each at a flow of 20 µL/min for 180 s. Data analysis was performed with the BIAevaluation 3.1.1 software (Biacore). The association constant k_a of a binding reaction is defined as [1/(M·s)] and the initial slope [RU/s] that follows the equation slope $\sim c \cdot k_a$ directly correlates with the concentration of the analyte. Data processing was performed using Prism 5.04 software (GraphPad). The mean determined slope [RU/s] of the unknown sample was applied to the determined standard curve algorithm (fit); the concentration was calculated thereof and multiplied by the dilution factor of the sample.

Detection of Serial Graft Tissue pO2 and Perfusion. The detailed methods for these procedures were recently published (34). Briefly, tissue oxygenation was measured using the OxyLab pO2 monitor (Oxford Optronix), and blood perfusion by laser doppler flowmetry using the OxyLab LDF monitor (Oxford Optronix). For FITC-lectin studies, whole-mount tracheas were evaluated for microvascular perfusion by fluorescence staining quantified by confocal microscopy as described (34).

Detection of Microvascular Permeability. Microvascular leakage in orthotopic tracheal transplants was assessed using a recently described protocol (8). Briefly, following FITC-lectin injection, 100 µL R50 Fluoro-Max red fluorescent microspheres, 0.048 µm in diameter (Thermo Scientific), were injected through the inferior vena cava. After 3–5 min in circulation, a sternotomy was performed, and the aorta was cannulated via the left ventricle with an 18-gauge angiocatheter and perfused with 1% paraformaldehyde for 3–5 min using a mini pump (Fisher Scientific). Grafts were harvested and mounted as described in the previous section. Microvascular permeability was assessed by using confocal microscopy to determine the extent of microsphere extravasation.

Immunofluorescence Staining and Detection of Thrombin. Grafts were harvested and embedded in Tissue-Tek optimum cutting temperature (OCT) compound (Sakura Finetek). A cryostat (HM550; Microm) was used to cut 6-µm sections of tracheal graft and the sections were placed on superfrost/plus slides (Fisher Scientific). After fixation in methanol/acetone (1:1) for 10 min at −20 °C, the slides were washed with PBS. Next, sections were blocked with 10% (vol/vol) donkey serum for 30 min and then incubated for 1 h either with rabbit anti-mouse C5b-9 (Abcam), rabbit anti-mouse tissue factor (American Diagnostic), goat anti-mouse C3d (R&D Systems), rat anti-mouse CD4 (BD Biosciences), rat anti-mouse CD8 (BD Biosciences), or with goat anti-mouse thrombin (Santa Cruz Biotechnology; sc 16972) and rat anti–mouse-CD31–specific (BD Biosciences) primary antibodies. The slides were washed with PBS, and sections were incubated with Alexa Fluor 488 donkey anti-rabbit, Alexa Fluor 488 donkey anti-goat IgG, Alexa Fluor 488 donkey anti-mouse IgG (Invitrogen), and Cy3 donkey anti-rat (Invitrogen) conjugated secondary antibodies. To demonstrate specificity of the thrombin deposition on vascular endothelial cells, tracheal sections were incubated for 60 min with 0.02 IU/mL hirudin (Sigma) in blocking solution before incubation with primary goat anti-mouse thrombin antibody. The sections were mounted with Vectashield mounting medium (Vector Laboratories) and analyzed by confocal microscopy. ImageJ software was used to quantitate emission wavelengths from the FITC-conjugated lectin, Cy3-conjugated secondary antibody used to detect CD31 antigen, and Alexa to detect thrombin deposition. The sections were mounted with Vectashield mounting medium (Vector Laboratories).

Quantification of Collagen. First, slides were stained by Picrosirius stain to detect collagen deposition in allografts as described previously (6) and imaged by Leica light microscope to localize collagen deposition. Five random high powered fields of orange/red band of collagen were captured per slide, and mean bandwidth of collagen in the subepithelium region was calculated by an automated software application, MetaMorph (Molecular Devices).

Statistical Analysis. GraphPad Prism software was used for statistical analysis. Differences between groups at multiple time points were compared using two-way ANOVA with Bonferroni multiple comparisons for post hoc analyses, whereas differences between single time points were compared by one-way ANOVA, and a P value <0.05 was considered significant.

1. Bishop GA, Waugh JA, Landers DV, Krensky AM, Hall BM (1989) Microvascular destruction in renal transplant rejection. *Transplantation* 48(3):408–414.
2. Matsumoto Y, McCaughan GW, Painter DM, Bishop GA (1993) Evidence that portal tract microvascular destruction precedes bile duct loss in human liver allograft rejection. *Transplantation* 56(1):69–75.
3. Luckraz H, et al. (2004) Microvascular changes in small airways predispose to obliterative bronchiolitis after lung transplantation. *J Heart Lung Transplant* 23(5):527–531.
4. Luckraz H, et al. (2006) Is obliterative bronchiolitis in lung transplantation associated with microvascular damage to small airways? *Ann Thorac Surg* 82(4):1212–1218.
5. Babu AN, et al. (2007) Microvascular destruction identifies murine allografts that cannot be rescued from airway fibrosis. *J Clin Invest* 117(12):3774–3785.
6. Jiang X, et al. (2011) Adenovirus-mediated HIF-1α gene transfer promotes repair of mouse airway allograft microvasculature and attenuates chronic rejection. *J Clin Invest* 121(6):2336–2349.
7. Sato M, Keshavjee S (2008) Bronchiolitis obliterans syndrome: Alloimmune-dependent and -independent injury with aberrant tissue remodeling. *Semin Thorac Cardiovasc Surg* 20(2):173–182.
8. Khan MA, et al. (2011) CD4+ T cells and complement independently mediate graft ischemia in the rejection of mouse orthotopic tracheal transplants. *Circ Res* 109(11):1290–1301.
9. Keshavjee S, Davis RD, Zamora MR, de Perrot M, Patterson GA (2005) A randomized, placebo-controlled trial of complement inhibition in ischemia-reperfusion injury after lung transplantation in human beings. *J Thorac Cardiovasc Surg* 129(2):423–428.
10. Huber-Lang M, et al. (2006) Generation of C5a in the absence of C3: A new complement activation pathway. *Nat Med* 12(6):682–687.
11. Segal JB, et al. (2001) Coagulation markers predicting cardiac transplant rejection. *Transplantation* 72(2):233–237.
12. Klussmann S, Nolte A, Bald R, Erdmann VA, Fürste JP (1996) Mirror-image RNA that binds D-adenosine. *Nat Biotechnol* 14(9):1112–1115.
13. Purschke WG, Eulberg D, Buchner K, Vonhoff S, Klussmann S (2006) An L-RNA-based aquaretic agent that inhibits vasopressin in vivo. *Proc Natl Acad Sci USA* 103(13):5173–5178.
14. Darisipudi MN, et al. (2011) Dual blockade of the homeostatic chemokine CXCL12 and the proinflammatory chemokine CCL2 has additive protective effects on diabetic kidney disease. *Am J Pathol* 179(1):116–124.
15. Vater A, Jarosch F, Buchner K, Klussmann S (2003) Short bioactive Spiegelmers to migraine-associated calcitonin gene-related peptide rapidly identified by a novel approach: tailored-SELEX. *Nucleic Acids Res* 31(21):e130.
16. Greinacher A, Warkentin TE (2008) The direct thrombin inhibitor hirudin. *Thromb Haemost* 99(5):819–829.
17. Raedler H, et al. (2011) Anti-complement component C5 mAb synergizes with CTLA4Ig to inhibit alloreactive T cells and prolong cardiac allograft survival in mice. *Am J Transplant* 11(7):1397–1406.
18. Rothberger H, Barringer M, Meredith J (1984) Increased tissue factor activity of monocytes/macrophages isolated from canine renal allografts. *Blood* 63(3):623–628.
19. Lin CC, et al. (2010) Recipient tissue factor expression is associated with consumptive coagulopathy in pig-to-primate kidney xenotransplantation. *Am J Transplant* 10(7):1556–1568.
20. Ji M, et al. (2011) The importance of tissue factor expression by porcine NICC in triggering IBMIR in the xenograft setting. *Transplantation* 91(8):841–846.

IMMUNOLOGY

21. Hölschermann H, et al. (2000) Hirudin reduces tissue factor expression and attenuates graft arteriosclerosis in rat cardiac allografts. *Circulation* 102(3):357–363.
22. Amara U, et al. (2010) Molecular intercommunication between the complement and coagulation systems. *J Immunol* 185(9):5628–5636.
23. Rutkowski MJ, et al. (2010) The complement cascade as a mediator of tissue growth and regeneration. *Inflamm Res* 59(11):897–905.
24. Polley MJ, Nachman R (1978) The human complement system in thrombin-mediated platelet function. *J Exp Med* 147(6):1713–1726.
25. Wetsel RA, Kolb WP (1983) Expression of C5a-like biological activities by the fifth component of human complement (C5) upon limited digestion with noncomplement enzymes without release of polypeptide fragments. *J Exp Med* 157(6):2029–2048.
26. Krisinger MJ, et al. (2012) Thrombin generates previously unidentified C5 products that support the terminal complement activation pathway. *Blood* 120(8):1717–1725.
27. Ward PA, Hill JH (1970) C5 chemotactic fragments produced by an enzyme in lysosomal granules of neutrophils. *J Immunol* 104(3):535–543.
28. Huber-Lang M, et al. (2002) Generation of C5a by phagocytic cells. *Am J Pathol* 161(5): 1849–1859.
29. Zwirner J, Fayyazi A, Götze O (1999) Expression of the anaphylatoxin C5a receptor in non-myeloid cells. *Mol Immunol* 36(13–14):877–884.
30. Allegretti M, et al. (2005) Targeting C5a: Recent advances in drug discovery. *Curr Med Chem* 12(2):217–236.
31. Woodruff TM, Nandakumar KS, Tedesco F (2011) Inhibiting the C5-C5a receptor axis. *Mol Immunol* 48(14):1631–1642.
32. DiScipio RG, Daffern PJ, Jagels MA, Broide DH, Sriramarao P (1999) A comparison of C3a and C5a-mediated stable adhesion of rolling eosinophils in postcapillary venules and transendothelial migration in vitro and in vivo. *J Immunol* 162(2):1127–1136.
33. Tsuji RF, et al. (2000) Early local generation of C5a initiates the elicitation of contact sensitivity by leading to early T cell recruitment. *J Immunol* 165(3):1588–1598.
34. Khan MA, Dhillon G, Jiang X, Lin YC, Nicolls MR (2012) New methods for monitoring dynamic airway tissue oxygenation and perfusion in experimental and clinical transplantation. *Am J Physiol Lung Cell Mol Physiol* 303(10):L861–L869.